Voltage Reduction and Lifetime Elongation of Organic Light-Emitting Diodes Using Photopolymerization for Fluorizated Polyxylylene Hole Injection Layer

2012 Jpn. J. Appl. Phys. 51 032101

(http://iopscience.iop.org/1347-4065/51/3R/032101)

Japanese Journal of Applied Physics **51** (2012) 032101 **REGULAR PAPER**
DOI: 10.1143/JJAP.51.032101

Voltage Reduction and Lifetime Elongation of Organic Light-Emitting Diodes Using Photopolymerization for Fluorizated Polyxylylene Hole Injection Layer

Meng-Dan Jiang, Tien-Lung Chiu[1*†], Pei-Yu Lee[1], Shun-Po Yang[1], and Hong-Cheu Lin[†]

Department of Materials Science and Engineering, National Chiao Tung University, Hsinchu 30010, Taiwan, R.O.C.
[1]*Department of Photonics Engineering, Yuan Ze University, Chungli 32003, Taiwan, R.O.C.*

Received September 9, 2011; accepted December 15, 2011; published online February 22, 2012

This study describes a novel method for manufacturing a hole injection layer of an organic light-emitting diode (OLED), comprising an ultraviolet (UV) reactive Br–fluorocarbon precursor (Br–CF_2–C_6F_4–CF_2–Br). The proposed method can be used to form a fluorizated polyxylylene film, demonstrating high repeatability on the anode as the hole injection layer of organic electroluminescent devices to enhance the hole injection, reduce the operating voltage of 1.2 V, and extend the operational lifetime by more than 150 times under a high current density of 125 mA/cm^2. Using a spin-coating process, the remaining precursor can be recycled to prevent wasting materials. UV curing without the solvent-removing process shortens manufacturing time. Hence, fabricating a high performance OLED using a simple, low-cost process is the aim of this study.

1. Introduction

Organic light-emitting diodes (OLEDs),[1)] applied in displays and lighting electronics, are currently receiving considerable attention due to the advantages of light weight, flexibility, self-emission, wide view angle, high luminance, efficiency, low drive voltage, and fast response time.[2,3)] The electro-optical (EO) performance of OLEDs is continually advanced by engineering the device structure, advancing the organic materials, or modifying the layer interfaces of the device. In particular, carrier transportation at interfaces among these layers is a crucial factor in EO device performance. One of them, the hole injection layer between the inorganic indium tin oxide (ITO) anode and organic layer, is a concern for poor driving voltage, illumination, and operational reliability.[4,5)] Therefore, several approaches have been employed to mitigate these concerns, such as raising the work function of the ITO anode using a chlorinating process,[6)] or employing an organic, inorganic or oxide buffer layer.[7–10)] For organic bases, a number of layers have been reported to adjust the work function of the ITO anode to improve the hole injection and achieve the carrier balance,[11)] which can be composed of, for example, fluorocarbon layers,[12)] plasma polymerized CF_x,[13,14)] ultraviolet (UV) irradiated CF_x,[15)] thermal-deposited poly(tetrafluoroethylene),[16)] evaporable fluoro-molecules,[17)] and chemical vapor deposited parylene.[18,19)] Here, we introduce a simple process to manufacture the fluorocarbon layer, based on parylene without using a vacuum process.

Parylene is the generic name for members of a unique xylylene polymer series developed during the past four decades for wide commercial applications in several fields of electronics, optoelectronics, integrated circuits, micro-electro-mechanical systems, and biomedical devices.[20,21)] Single or multi parylene thin films, poly(*para*-xylylene) (–CH_2–C_6H_4–CH_2–, PPX) or PPX-N, as environmental passivation layers for OLED applications have also been widely studied.[22)] In addition, PPX-N film (without fluorinating) was employed as a hole injection layer, and inserted between the hole transport layer and the ITO anode to reduce the occurrence of dark spots caused by the ion diffusion,[19)] and to improve the hole injection from ITO anode into the organic hole transport layer. Although the PPX-N films typically exhibit poor thermal stability above the temperature of 400 °C, they can be improved by fluorinating the dimer of *p*-xylylenes.

A commercial fluoride parylene derivative PPX demonstrates unique properties, including higher dielectric strength, higher temperature integrity, a lower dielectric constant, a lower coefficient of friction, and higher mechanical strength compared to that of the original parylene. Fluoride PPX derivatives can be employed in fluorocarbon polymer film, such as PPX-F (–CF_2–C_6H_4–CF_2–) and perfluoro-PPX (–CF_2–C_6F_4–CF_2–). In general, the process for manufacturing fluorocarbon polymer film involves evaporating parylene dimers at a temperature between 100 and 200 °C, and then undergoing pyrolysis by entering a thermal cracker at a high temperature between 600 and 750 °C.[21)] These gaseous intermediates used as radical monomers are introduced into a deposition chamber with a high vacuum to form a fluorocarbon polymer thin film as a buffer layer of organic light-emitting diodes (OLEDs). However, certain disadvantages exist in using this complex process to form a fluorocarbon film, such as expensive and intricate manufacturing equipment, additional costs for maintenance and replacement of reactors, and waste of materials.

Hence, a fluorizated polyxylylene (FPX) film used as a buffer layer is employed as a hole injection layer on the anode to improve the smoothness, durability, and adhesion of ITO. Such a film enhances the hole injection, reduces the operating voltage and improves the operating stability to enhance the performance of the OLED. However, no previous studies have reported such a UV-reactive fluoro-precursor used to form a fluorizated polymer film on an anode as a hole injection layer.

2. Experimental Methods

This study fabricated a buffer layer of FPX film on an ITO substrate to be the hole injection layer of an OLED. The sheet resistance of an ITO substrate is 13 Ω/□. The manufacturing process of FPX film involved spin-coating the liquid Br–fluorocarbon precursor (Br–CF_2–C_6F_4–CF_2–Br) on a pre-cleaned and patterned ITO substrate at 3,000 rpm and then curing by a UV illumination. In addition, after coating, the remaining Br–fluorocarbon precursor could

*E-mail address: tlchiu@saturn.yzu.edu.tw
†These authors contribute to this work equivalently.

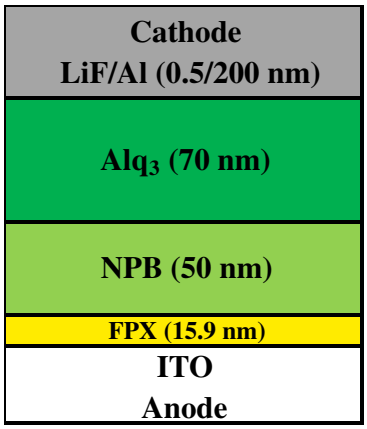

Fig. 1. (Color online) OLED configuration.

be recycled, and the conventional spin-coating process of removing solvents was unnecessary, preventing the problem of waste. The UV exposure energy was set to 500 mJ/cm^2. Through exposure to UV light, the Br–fluorocarbon precursor could be cured to form a fluorocarbon polymer film with a thickness of 15.9 nm. The workfunction, transparency, morphology and thickness of the FPX film were examined utilizing a photoelectron spectrometer (Riken Keiki AC-2), UV–visible spectrometer (Hitachi U4100) and atomic force microscopy (AFM; Seiko SPA400).

Subsequently, various thin films were deposited on the FPX-modified ITO (FPX-ITO) using a thermal sublimed evaporator under a high vacuum pressure of 2×10^{-6} Torr. As shown in Fig. 1, the detailed configuration of our device comprised an ITO anode, FPX film as the hole injection layer, *N*,*N*′-bis(naphthalen-1-yl)-*N*,*N*′-bis(phenyl)benzidine (NPB) as the hole transport layer, tris(8-hydroxyquinoline)aluminum (Alq_3) as both the emitting and electron transport layer, lithium–fluoride (LiF) as the electron injection layer, and an aluminum (Al) cathode. These materials were purchased from Uni-Onward, with larger than 99.5% purity. The deposited film thicknesses were 50, 70, 0.5, and 200 nm for NPB, Alq_3, LiF, and Al, respectively. In particular, the deposition rate of the organic layers (NPB and Alq_3), LiF, and Al were controlled at approximately 2.5, 0.1, and 5 Å/s, respectively. The active area of the device was 0.04 cm^2. Furthermore, a reference OLED was fabricated using the previously discussed process, except for the step involving FPX lamination. The devices were carefully encapsulated in a glove box and their current–voltage (*J*–*V*) and luminance–voltage (*L*–*V*) characteristics were obtained in room temperature by using an electrical and optical measurement system consisting of a source meter (Keithley 2400) and a photometer (Minolta CS1000).

3. Results and Discussion

Because some difficulties related to short circuits and trap-induced interface barriers of carrier dynamics frequently originate from the spikes and defects on the surface of ITO substrates, the morphology on the ITO surface is an importation factor affecting the electroluminescent (EL) characteristics of OLED devices. Hence, we used AFM to imitate the three-dimensional morphologies on the surface of

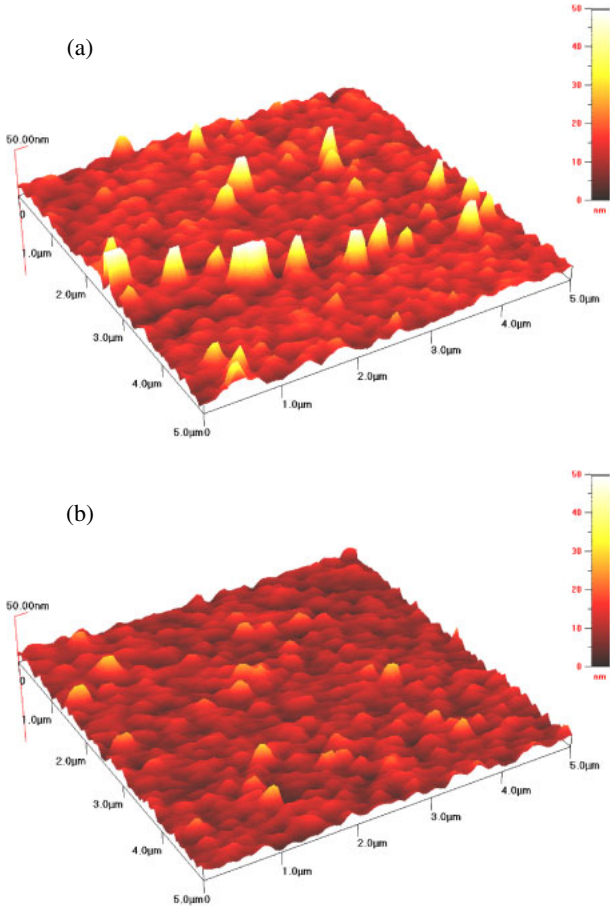

Fig. 2. (Color online) AFM images with a scanning area of $5 \times 5\,\mu m^2$ for (a) FPX-modified ITO and (b) bare ITO.

the bare ITO and FPX-ITO, as shown in Fig. 2. The scan area was $5 \times 5\,\mu m^2$, and the root-mean-square roughness (R_{rms}) of FPX-ITO and bare ITO were determined to be 3.33 and 4.99 nm, respectively. The morphology changed significantly from irregular and uneven spikes to homogenous and smooth films by spin-coating the FPX film. Because the height of the original spikes was approximately 40 nm, it was reduced to approximately 24 nm after leveling bare ITO using 15.9 nm FPX lamination. Most parts of the small spikes disappeared. This ensured that the defects or spikes on the ITO surface were eliminated, and that the difficulties related to short circuits and trap-induced interface barriers of carrier dynamics in the devices were also prevented.

Particularly, the FPX layer also exhibited excellent transparency measured using a UV–visible spectrometer as shown in Fig. 3. In the visible band from 400 to 700 nm, the transmittance of FPX-ITO is better than that of the bare ITO because of its graded refractive index structure. The reflection at ITO/air interface is reduced by FPX layer, corresponding to increasing transmission. At 550 nm, the maximum human visual sensitivity, FPX-ITO performs 88% higher transmittance than that of bare ITO (85%), which is conducive to the light output of EL devices. These two substrates were also employed to measure the photoelectron spectrum for investigating their workfunction as shown in the inset of Fig. 3. The workfunction of FPX and ITO was 5.25 and 4.9 eV, respectively. Hence, FPX formation not only smoothed the surface, but also raised the transmittance

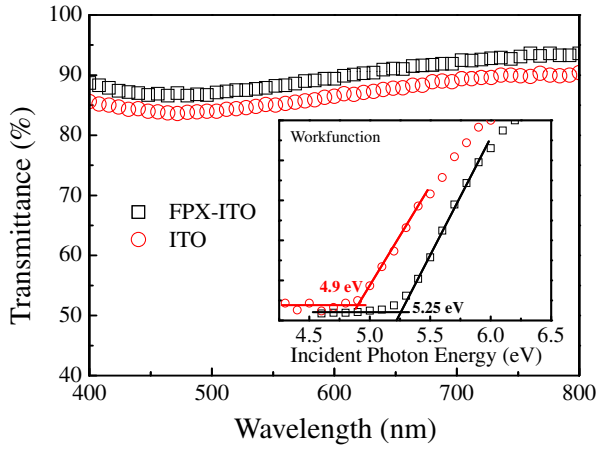

Fig. 3. (Color online) Transmittance spectrum and photoelectron spectrum (inset) of FPX and bare ITO.

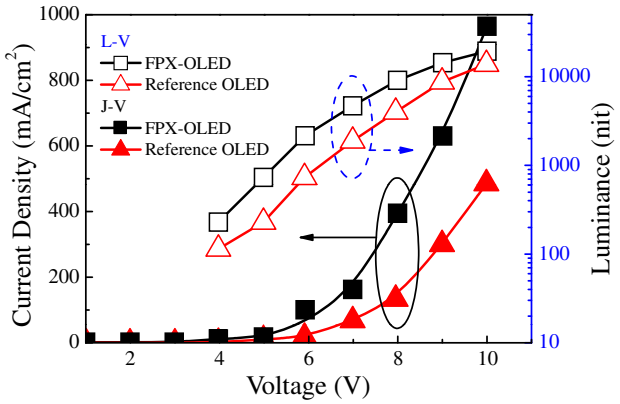

Fig. 4. (Color online) *L*–*J*–*V* characteristics of FPX- and reference OLED.

and workfunction. Both FPX-ITO and bare ITO contribute to the improvement of EO characteristics of OLED devices.

Figure 4 shows the *J*–*V* and *L*–*V* curves of two green OLEDs fabricated on the FPX-ITO and bare ITO (as a reference device). The OLED, with an additional 15.9-nm-thick FPX film formed between the ITO and NPB, has a more favorable *J*–*V* curve and sharper forward biased diode behavior, in comparison to the reference OLED. This implies that the FPX layer not only balances the energy barrier between the ITO and NPB, but also enhances the hole injection to achieve the charge balance, resulting in a substantial decrease of driving voltage and sharper forward biased diode behavior.[23] Reasonably, the FPX-OLED shows higher *L*–*V* performance, attributed to the charge balance and corresponding to more exciton and photon formations, which also implies more photons coupling out of the emitting layer. In addition, the higher transmittance of FPX-ITO facilitates the photon emitting out of devices to increase the luminance. At a low current density of 15 mA/cm^2, which is the general operational current density of OLEDs, the driving voltages are 5 and 5.46 V, the luminance levels are 741 and 448 cd/cm^2, and the current efficiencies are 4.94 and 2.99 cd/A for the FPX-OLED and reference OLED. However, the current efficiency of the FPX-OLED decayed more rapidly than did the reference OLED, as the current

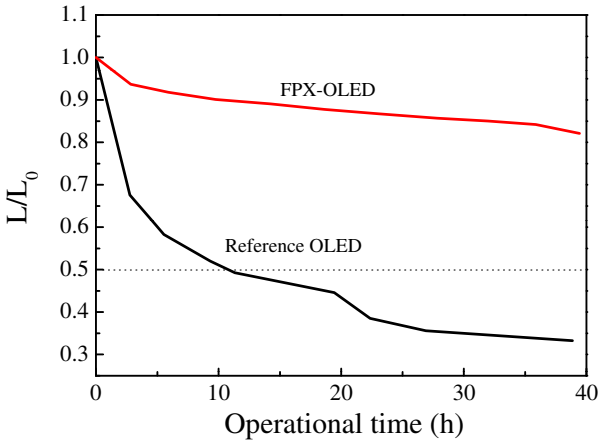

Fig. 5. (Color online) Accelerated operational lifetime of FPX-OLED and reference OLED by applying a constant current density of 125 mA/cm^2.

density increased. Finally, the current efficiencies of the FPX-OLED and reference OLED at high current densities (over 100 mA/cm^2) are nearly identical because of the bottlenecks of charge unbalance and Alq_3^+ accumulation at the emitting layer.[24]

An extremely high and steady current density of 125 mA/cm^2 was applied to a rapidly aging OLED to evaluate the operating stability of OLEDs with the FPX-ITO and the bare ITO, as shown in Fig. 5. The driving voltages and initial brightnesses (L_0) of the FPX-OLED and reference OLED were 7.7 and 6.5 V, and 3575 and 3700 cd/m^2, respectively. The diminution in the brightness of the FPX-OLED is not consequential after long-term operation, but the brightness of the comparative OLED decreases by half after 10.7 h of operation. We simulated the decaying trend of the final 10 h to calculate the half-life time of the FPX-OLED, which is more than 1,500 h. In addition, we also observed that the growth rate of the dark spot on the FPX-OLED is slower than that of the reference OLED, similar to the results reported by Ke *et al.*[19] Therefore, FPX film is a critical factor for enlarging the operational reliability of OLEDs. Here, thin fluorocarbon polymer FPX films demonstrate several advantageous uses, such as smoothing the morphology of the ITO surface, inhibiting the metal migration, blocking the permeation of oxygen and moisture to reduce the occurrence of dark spots, achieving carrier balance and increasing the lifetime of the devices.

4. Conclusions

This study successfully introduces a UV-reactive Br–fluorocarbon precursor to form a fluorocarbon FPX film on the anode to reduce the operating voltage, improve the operating stability, and enhance the EO performance of OLED devices. These are caused from the FPX film smoothing the surface morphology of bare ITO, preventing the formation of traps and spikes, blocking the permeation of contamination to elongate the operational lifetime, and improving the hole injection. In addition, the method for manufacturing this FPX film is a simple and repeatable spin-coating process. The cost of this FPX film can be low because the precursor can be recycled, the material can be saved, and the process of removing the solvent is unnecessary, thus saving time.

Acknowledgments

The authors would like to thank National Science Council (NSC) and Chung-Shan Institute of Science and Technology (CSIST) of Taiwan for financial support under Grant Nos. NSC 99-2622-E-155-010-CC3, 99-2221-E-155-092, 100-2622-E-155-008-CC3, and 100-2221-E-155-046 as well as using the facilities in CSIST.

1) C. W. Tang and S. A. Vanslyke: Appl. Phys. Lett. **51** (1987) 913.
2) Y. Sun and S. R. Forrest: Nat. Photonics **2** (2008) 483.
3) T. L. Chiu, P. Y. Lee, J. H. Lee, C. H. Hsiao, M. K. Leung, C. C. Lee, C. Y. Chen, and C. C. Yang: J. Appl. Phys. **109** (2011) 084520.
4) T. Kugler, M. Lögdlund, and W. R. Salaneck: IEEE J. Sel. Top. Quantum Electron. **4** (1998) 14.
5) M. D. Jiang, P. Y. Lee, T. L. Chiu, H. C. Lin, and J. H. Lee: Synth. Met. **161** (2011) 1828.
6) M. G. Helander, Z. B. Wang, J. Qiu, M. T. Greiner, D. P. Puzzo, Z. W. Liu, and Z. H. Lu: Science **332** (2011) 944.
7) Z. Liu, M. G. Helander, Z. Wang, and Z. Lu: J. Phys. Chem. C **114** (2010) 16746.
8) J. Cui, Q. Huang, J. C. G. Veinot, H. Yan, Q. Wang, G. R. Hutchison, A. G. Richter, G. Evmenenko, P. Dutta, and T. J. Marks: Langmuir **18** (2002) 9958.
9) L. Niu and Y. Guan: Phys. Status Solidi A **207** (2010) 993.
10) P. Stakhira, V. Cherpak, D. Volynyuk, F. Ivastchyshyn, Z. Hotra, V. Tataryn, and G. Luka: Thin Solid Films **518** (2010) 7016.
11) C. Ganzorig, K. J. Kwak, K. Yagi, and M. Fujihira: Appl. Phys. Lett. **79** (2001) 272.
12) K. Okumoto, H. Kanno, Y. Hamaa, H. Takahashi, and K. Shibata: Appl. Phys. Lett. **89** (2006) 063504.
13) L. S. Hung, L. R. Zheng, and M. G. Mason: Appl. Phys. Lett. **78** (2001) 673.
14) M. F. Lo, T. W. Ng, S. L. Lai, M. K. Fung, S. T. Lee, and C. S. Lee: Appl. Phys. Lett. **99** (2011) 033302.
15) S. W. Tong, C. S. Lee, Y. Lifshitz, D. Q. Gao, and S. T. Lee: Appl. Phys. Lett. **84** (2004) 4032.
16) Y. Gao, L. Wang, D. Zhang, L. Duan, G. Dong, and Y. Qiu: Appl. Phys. Lett. **82** (2003) 155.
17) D. Q. Gao, M. Y. Chan, S. W. Tong, F. L. Wong, S. L. Lai, C. S. Lee, and S. T. Lee: Chem. Phys. Lett. **399** (2004) 337.
18) S. J. Chua, L. Ke, R. S. Kumar, and K. Zhang: Appl. Phys. Lett. **81** (2002) 1119.
19) L. Ke, R. S. Kumar, K. Zhang, S. J. Chua, and A. T. S. Wee: Synth. Met. **140** (2004) 295.
20) C. Y. Lee, G. W. Wu, and W. J. Hsieh: Sens. Actuators A **147** (2008) 173.
21) C. M. Chou, K. C. Hsieh, C. J. Chung, and J. L. He: Surf. Coatings Technol. **204** (2010) 1631.
22) L. Zhou, A. Wanga, S. C. Wu, J. Sun, S. Park, and T. N. Jackson: Appl. Phys. Lett. **88** (2006) 083502.
23) R. Meerheim, S. Scholz, S. Olthof, G. Schwartz, S. Reineke, K. Walzer, and K. Leo: J. Appl. Phys. **104** (2008) 014510.
24) A. Pinato, N. Wrachien, M. S. Weaver, J. J. Brown, and G. Meneghesso: IEEE Trans. Electron Devices **57** (2010) 178.